QUANTIFYING THE DEGRADATION OF GLASS FIBER REINFORCED POLYMERS UNDER WEATHERING CONDITIONS: A MICRO-SCALE MODELING APPROACH

M. Kucher[1], P. Johst[1], M. Lizaranzu[2], F. Lahuerta[2] and R. Böhm[1]

[1] Faculty of Engineering, Leipzig University of Applied Sciences, Leipzig, Germany, michael.kucher@htwk-leipzig.de, philipp.johst@htwk-leipzig.de, robert.boehm@htwk-leipzig.de

[2] Instituto Tecnológico de Aragón (Itainnova), Zaragoza, Spain, flahuerta@itainnova.es, mlizaranzu@itainnova.es

Keywords: Composite; epoxy resin, moisture absorption; property deterioration; representative volume element (RVE); temperature dependency; ultraviolet (UV) radiation

ABSTRACT

Glass fiber reinforced polymers (GFRP) are widely used as composite material for a variety of applications such as wind turbine blades (WTBs). During their operating time, these GFRP structures are exposed to natural weathering conditions, such as low and elevated temperatures, ultraviolet radiation and moisture. These weathering phenomena influence the material's mechanical properties due to material aging and the degradation of the composite's mechanical properties. For a reliable lifetime assessment and the design of a repurposed application of WTBs, the quantification of GFRP's degradation is required. For this reason, the aim of the current study is to numerically estimate the combined effects of weathering on the mechanical properties of GFRP. Therefore, the effective elastic properties of a unidirectional GFRP composite were determined considering representative volume elements. The required numerical modelling was performed using finite element analysis. The mechanical properties of glass fibers, epoxy resin and their relationship with individual natural aging phenomena were used based on the existing literature values. As a result of the micro-scale modeling, the change of temperature and moisture absorption have the highest effect on the elastic properties on the epoxy resin and thus also on the GFRP composite. The used numerical approach enables a preliminary estimation of environmental-based degradation phenomena of GFRP which can be used at an early stage of developments of composite structures, the reuse of composites or for planning experimental studies considering degradation of these composite materials.

1 INTRODUCTION

Glass fiber reinforced polymers (GFRP) are one of the most widely used composite materials and are e.g. chosen as material for wind turbine blades (WTBs). The life time of onshore wind turbines is typically approximately 20 years [1]. During this time, wind turbines, especially the WTBs, are exposed to natural weathering conditions, such as changing temperatures, ultraviolet (UV) radiation and moisture exposure. These weathering phenomena result in aging and degradation of the composite materials used [2]. Thereby, the term degradation describes all processes which lead to a decline of polymer's and composite's properties; and the term aging denotes a long-term change of polymer properties and may involve degradation processes [3]. The different weathering conditions result in degradation, aging and could change the morphology of the GFRP [4]. The degradation of polymers and polymer based composites starts at the outer surface and gradually penetrates into the interior of the material [3] (Figure 1). To avoid the negative influence of different weathering phenomena, the surfaces of WTBs are protected with gelcoat or paint [2, 5]. In the near-surface regions and in the case of a missing coating, all kinds of weathering phenomena lead to a change of the composite's mechanical material properties. The exposure to ultraviolet (UV) radiation may cause significant degradation of polymeric materials (see references [6, 7]). UV light has the ability to damage the composite's polymeric surface, exposing the fibers and boosting water absorption [7]. Most of the solar radiation is classified as UV-B which is filtered by the stratosphere and therefore does not reach the earth's surface. The solar radiation UV-A has a wavelength of 315 to 400 nm and reaches the surface of the earth. It results in photochemical degradation of polymeric materials [3]. The term photochemical degradation is denoted as the degradation of photodegradable molecules caused by the absorption of photons from sunlight [3]. Furthermore, WTBs are exposed to water in the form of steam due to the humidity of air and soil moisture or in the form of liquid water due to precipitation in the form of rain or snow. The presence of moisture can lead to degradation of mechanical properties, especially in non-surface treated GFRP. The combined influence of temperature and moisture ingression, particularly in combination with fatigue loading may impact the mechanical properties of composite materials [8, 9]. This effect is described as hydrothermal degradation.

In the literature, there are several experimental studies focusing the individual or combined effect of changing temperature, UV radiation and moisture on the mechanical properties of composites [7, 10–16]. Bazil et al. analyzed the resulting ultimate strength of different configuration of GFRP laminates for different environmental conditions including freeze and thaw cycles with and without the presence of moisture, UV radiation and water vapor condensation [12]. They further investigated the degradation of GFRP pultruded profiles after exposure to various weathering cycles using bending, tensile and compression tests [11]. Dogan et al. figured out that coated materials are less sensitive to hygrothermal strength degradation than uncoated composite materials [10]. Shin et al. investigated the correlation of accelerated aging test to natural aging test on graphite-epoxy composite materials [13]. Martins carried out a comparative study of the phenomenological behavior of silica-polytetrafluoroethylene matrix reinforced composite before and after accelerated ageing with exposure to UVB radiation and water vapor [14]. Mouzakis et al. performed dynamic mechanical analysis (DMA) for a range of temperatures and frequencies under tensile and three-point bending loadings of glass fiber reinforced polyester and revealed that the aged material's stiffness increases, whereas a small deterioration in the composite's strength was determined [15]. Sousa et al. analyzed the mechanical properties of pultruded profiles made of E-glass fiber reinforced vinylester and polyester and compared different accelerated exposures to natural weathering in a Mediterranean climate [16]. These experimental studies largely represent the mechanical behavior of composites before and after accelerated exposure, natural weathering or both, but do not cover the full range of weathering conditions which are required for the assessment of composite applied in WTBs. Furthermore, the investigation did not only focus on glass fiber reinforced epoxy resins.

To overcome the lack of knowledge concerning the elastic properties of composites under accelerated exposure or natural weathering, a micro-scale modeling approach is used in the current study. For consideration including fiber misalignment or an inelastic material behavior of composites' components, numerical micro-scale modeling provide more accurate results [17]. In this context, finite element analyses (FEA) are particularly widespread. Therefore, the micro structure of the composite material is described by means of representative volume element (RVE). The mechanical properties of the individual components and the boundary layer are modeled and the effective properties of the composite are calculated numerically with the aid of a suitable homogenization technique. This micro-scale modeling allows a fast and effective investigation of different fiber arrangement and fiber volume ratios which can be used to assess the structural behavior of composite structures. Furthermore, it enables a better design, lifetime assessment of WTBs and the quantification of GFRP's degradation. This information allows an assessment of WTB's structural integrity, a decision on life extension and planning for the decommissioning of WTBs in the sense of a circular economy system (compare e.g. [18]). Furthermore, this quantification of the composite's mechanical properties at their end-of-life (EoL) enable the choice of suitable waste-treatment strategies, such as the so-called R6-strategy [19].

Due to the lack of experimental data considering the dependencies of all relevant weathering phenomena and for the required range of weathering conditions, the aim of the current study is to numerically investigate the elastic property's degradation of glass fiber reinforced epoxy resin according to changing temperatures within the relevant temperature range, moisture absorption and the exposure of UV radiation. Using a numerical micro-scale modeling approach, the dependencies of these phenomena on the composite effective elastic properties are estimated and analyzed. Therefore, the elastic properties of the composite were determined using a finite elements analysis of the composite's micro structure. Based on available literature values, the degradation of E-glass fiber and cold-curing epoxy resin according to the individual weathering conditions was quantified. Using these elastic properties of the composite's components, the elastic properties of the composite were estimated. A set-theoretic accumulation approach for the determination of the composite component's degradation was applied. Finally, the composite's resulting elastic constant of the UD reinforced GFRP and their degradation according to changing temperatures, moisture absorption and UV radiation was numerically investigated. Using suitable experimental data including all considered weathering phenomena and the interactions, the used micro-scale modeling approach can be used to quantify the degradation of glass fiber reinforced polymers under weathering conditions.

2 MATERIALS AND METHODS

2.1 Wind turbine blade and visual damage analysis

A segment of a WTB (E-40, Enercon, Aurich, Germany) with the dimensions of approximately 1.1 mm in width direction and 2.0 mm in length direction was used for the identification of typical damages [20–23]. The decommissioned blade was segmented with the help of an industrial excavator using a wire saw. Before the visual inspection, soiling caused by storage was removed and the segment was cleaned with a mild soap solution. After the segment was completely dried, the entire surface was inspected visually and individual damages were documented including length scales of the individual damages.

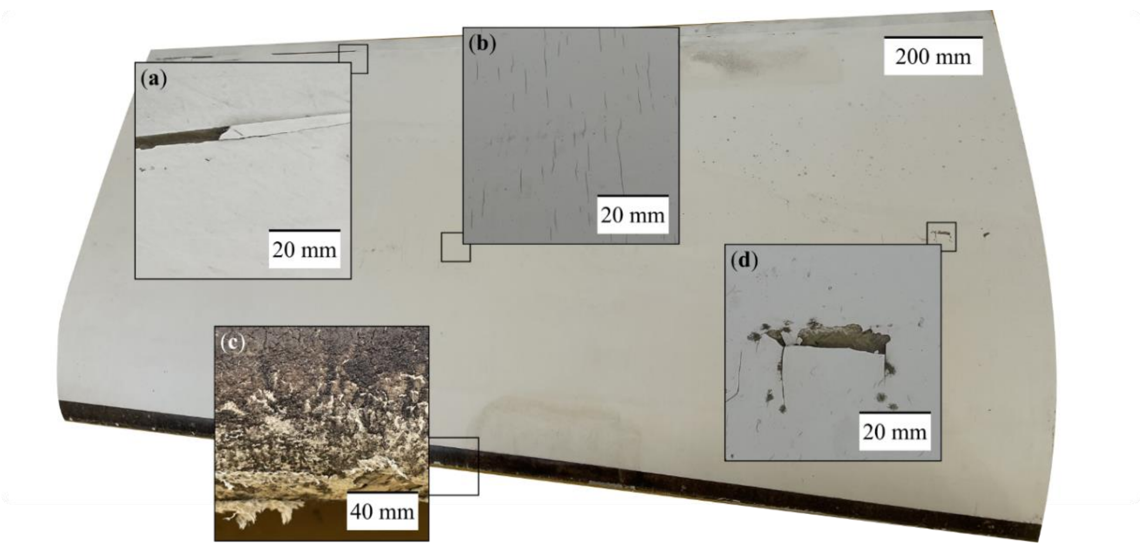

Figure 1: Segment of a decommissioned E-40 wind turbine blade with different kinds of damages, (**a**) shell debonding tail edge, **(b**) gelcoat cracks, (**c**) leading edge erosion, (**d**) mechanical damage.

Typical damage, such as shell debonding tail edge, gelcoat cracks, leading edge erosion, mechanical damage, could be detected in the examined WTB segment (Figure 1). In particular, damage to the surface coating allows moisture to penetrate the structure and thus alter the mechanical properties of the outer laminates.

The dimensions of the available WTB segment (Figure 1) was manually measured by means of different length measures. Based on these measurements, the generation of the three-dimensional model was carried out using the multi-platform software suite (CATIA V5-6R2018, Dassault Systems, Velizy-Villacoublay, France). For the consideration of the cross-sectional dimensions of the WTB, a scaled sectional view of the composite structure including the WTB's individual materials was generated (Figure 2b). This cross-section was used for the set-theoretical accumulation approach of the individual weathering phenomena presented in the following.

2.2 Set-theoretical accumulation approach of the different weathering phenomena

The individual weathering conditions according to changing temperatures, UV radiation and moisture absorption influences the material properties of the used composite materials. In practice, there can be interactions between these phenomena which have to be intensively examined. One possible approach to define these interactions is a set-theoretical accumulation (Figure 2a). Each weathering condition represents its own set, defined as set E, set R and set M for the changing temperatures, moisture absorption and UV radiation, respectively. According to basic set-theoretical considerations, different combinations of this conditions can be defined (compare Figure 2a).

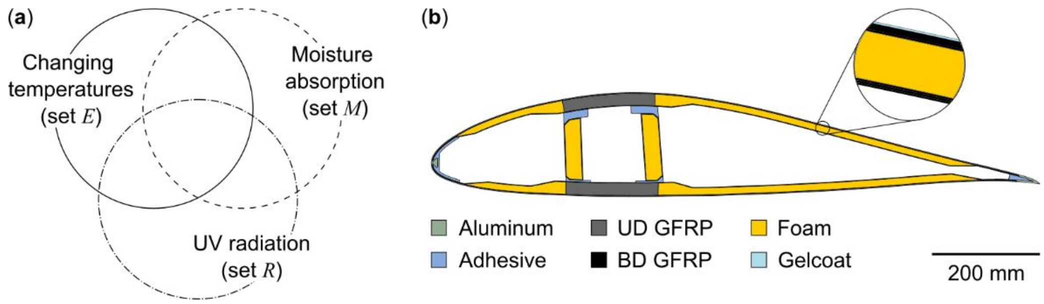

Figure 2: (**a**) Set-theoretical accumulation of individual weathering conditions and (**b**) cross-section of wind turbine blade at andthe used material components.

The gelcoats used as coating of WTBs are exposed to all weathering phenomena (compare e.g. [2, 5]). In the case that this protection layer is destroyed due to damages (Figure 1), the outer layers consisting of bidirectional (BD) reinforced epoxy resin are exposed to all weathering conditions including changing temperatures, moisture absorption and UV radiation (Figure 2a, area $E \cap M \cup R$). Since these areas are considerable small, the full combination of changing temperatures, moisture absorption and UV radiation has only a small effect on the structural behavior. More relevant for the resulting elastic behavior of WTBs is the interaction of moisture absorption due to precipitations and changing temperatures (Figure 2a, area $E \cap M \backslash R$). This affects in particular the outer BD reinforced layers. For a constant temperature distribution over the entire cross-section, the remaining inner materials are only exposed to changing temperatures (Figure 2a, area $E \backslash (R \cup M)$.

2.3 Numerical micro-scale modeling

To determine the effects of the degradation of the individual components on the effective properties of the composite and for the sake of simplicity, a UD laminate is analyzed. Therefore, the following subscripts f is used for the glass fibers, m for the epoxy resin matrix and c for the resulting composite. The fiber volume ratio φ is defined as $\varphi = V_{\mathrm{f}}/V_{\mathrm{c}}$. Using a numerical micro-scale modeling approach, the composite's effective elastic constants of the composite are obtained. For the considered transversely isotropic linear elastic material behavior, the strain stress relation can be written in the Voigt notation [24, 25]

$$\underbrace{\begin{bmatrix} \varepsilon_1 \\ \varepsilon_2 \\ \varepsilon_3 \\ \gamma_{23} \\ \gamma_{31} \\ \gamma_{21} \end{bmatrix}}_{\underline{\varepsilon}} = \underbrace{\begin{bmatrix} \frac{1}{E_{||}} & \frac{-\nu_{\perp||}}{E_{||}} & \frac{-\nu_{\perp||}}{E_{||}} & 0 & 0 & 0 \\ \frac{-\nu_{\perp||}}{E_{||}} & \frac{1}{E_{\perp}} & \frac{-\nu_{\perp\perp}}{E_{\perp}} & 0 & 0 & 0 \\ \frac{-\nu_{\perp||}}{E_{||}} & \frac{-\nu_{\perp\perp}}{E_{\perp}} & \frac{1}{E_{\perp}} & 0 & 0 & 0 \\ 0 & 0 & 0 & \frac{2(1+\nu_{\perp\perp})}{E_{\perp}} & 0 & 0 \\ 0 & 0 & 0 & 0 & \frac{1}{G_{\perp||}} & 0 \\ 0 & 0 & 0 & 0 & 0 & \frac{1}{G_{\perp||}} \end{bmatrix}}_{\underline{\underline{S}}} \underbrace{\begin{bmatrix} \sigma_1 \\ \sigma_2 \\ \sigma_3 \\ \tau_{23} \\ \tau_{31} \\ \tau_{21} \end{bmatrix}}_{\underline{\sigma}} \tag{1}$$

consisting of engineering constants denoted by $||$ for the fiber's longitudinal direction and $\perp$ for the transversal direction. This yields the longitudinal modulus $E_{||}$, the transversal modulus $E_{\perp}$, the shear modulus $G_{\perp||}$ in the orthogonal plane, the Poisson's ratio $\nu_{\perp||}$ due to longitudinal elongation, the Poisson's ratio $\nu_{\perp\perp}$ due to transversal elongation and shear modulus $G_{\perp\perp}$ in the isotropic plane (compare e.g. [24, 25]). In Eq. (1) $\underline{\varepsilon}$ is the strain vector, $\underline{\underline{S}}$ is the compliance matrix and $\underline{\sigma}$ is the stress vector. To determine the five engineering constants, the numerical micro-scale modeling approach is carried out by means of a simulation software (Ansys 2019 R2, Ansys, Canonsburg, Pennsylvania, United States). For the considered small dimensions of the RVEs, volume loads were neglected. Furthermore, the following modeling assumptions for a UD composites were assumed according to reference [26]:

- The fiber volume ratio has a constant value.
- The composite consists of isotropic linear-elastic matrix and fiber materials (Table 1).
- The fibers have an infinite length and are ideal cylindrical with a constant fiber diameter of d_{f}.
- There is a perfect bonding between the fibers and matrix material.
- All fibers are perfectly oriented in longitudinal direction without any misalignment.
- Periodic boundary conditions are defined for the RVE.

Taking the degradation of fibers' and polymeric matrix' stiffness into consideration, the resulting degraded elastic properties of UD composite were determined. For E-glass fibers and cold-curing epoxy resin, generally valid material parameters and not the material parameter of a certain supplier were used according to Schürmann et al. [25].

Properties	$\boldsymbol{E}$ in MPa	$\boldsymbol{\nu}$ -	$\boldsymbol{\rho}$ in g cm^{-3}
Epoxy resin, cold-curing	3150	0.37	1.19
E-glass fiber	73000	0.22	2.54

Young's modulus E, Poisson's ratio ν, mass density ρ

Table 1: Mechanical properties of epoxy resin and E-glass fiber according to reference [25].

In order to exclude an influence of the micro structure on the resulting mechanical properties, the Monte Carlo method of different fiber arrangements was used and the mean values of the individual simulation were calculated. The random fiber distribution was generated using the sequential addition and migration method according to Schneider [27] which considers a repeated count c_{RVE} of the geometry. Using the tool 'Material Designer', the FEA software periodic and conformal meshes were automatically generated to ensure the assumptions of periodic RVEs. As elements, SOLID187 elements were used (Figure 3) which have a quadratic displacement behavior and are well suited for the modeling of irregular meshes. For the considered fiber volume ratio of φ = 0.572, a fiber diameter of d_f = 15 µm and a repeat count of c_RVE = 5, the resulting RVEs consist of a number of 26 glass fibers and had the main dimensions of 179 µm × 90 µm × 90 µm. In this RVE, all fibers are oriented in x_1 direction (compare Figure 3).

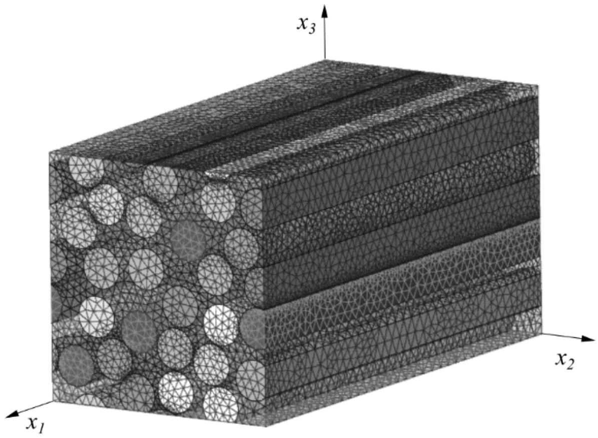

Figure 3: Resulting RVE of the investigated unidirectional composite (GFRP) with a fiber volume ratio of φ = 0.572.

2.4 Data collection procedure of stiffness degradation

The stiffness degradation of the E-glass fibers and of the polymer matrix epoxy resin according to the weathering phenomena changing temperatures, UV radiation and moisture was taken from different literature sources. This approach was applied since no referenceable data of the resin systems and glass fibers used were available. The measured data was determined by digitizing the existing diagrams. Since the properties of the particular kind of used epoxy resin vary due to the wealth of different resin systems, hardener contents and processing parameters, only the relative changes of the properties according to the individual weathering phenomena were examined for polymer matrix. Analogously, this consideration was used for the properties of glass fibers. Therefore, an initial elastic modulus E_0 at 20 °C, not exposed to UV radiation and completely dry was considered as reference value, respectively. Using this value, the relative changes of materials' elastic properties were quantified (Figure 4). This approach enables the comparison of the different individual weathering phenomena in terms of their magnitude and the usage of the exiting experimental data.

For the micro-scale modeling, the degradation of the elastic properties according to moisture absorption for a relative humidity of 60 % was analyzed in dependency of the time t. The change of stiffness properties was related to the ambient temperatures ϑ which were considered in the range between -50 °C and 70 °C [2]. The photochemical degradation was affected by the time t exposed to UV light. The time dependent effects of changing stiffness $E(t)$ were linearly interpolated between the existing data points using the numerical computing software (MATLAB version 9.12.0, MathWorks, Natick, Massachusetts, USA). This data was used to explain the material's stiff degradation for the individual phenomena which are required for the determination of the composite's stiffness as described in Section 2.1. Using the stiffness degradation and the elastic properties of the composite components (Table 1), the engineering constants of the compliance matrix in Eq. (1) were determined. The determined data sets and their related references are presented in the following.

According to the set-theoretical accumulation (compare Section 2.2), the change of the composite components' elastic properties to all individual weathering phenomena is required. For this purpose, it was assumed in the current study that the individual effects accumulate and that interactions between the individual effects neither lead to an increase nor to a decrease of the resulting degradation. Considering the sets mentioned in Section 2.2 as subscripts E, M and R, the resulting degradation represented by the damage parameter (compare e.g. [28]) $D = (E_0 - E)/E_0 = \Delta E/E_0$ of the polymer matrix and the reinforcement fibers are denoted as

$$D_m = D_{E,m} + D_{M,m} + D_{R,m}, \quad (2)$$

$$D_f = D_{E,f} + D_{M,f} + D_{R,f}, \quad (3)$$

where D_E , D_M and D_R are of degradation values according to changing temperatures, moisture absorption and UV radiation. Using Eq. (2) and Eq. (3), the components' elastic properties for the numerical calculations were determined.

3. RESULTS AND DISCUSSION

3.1 Individual stiffness degradation of fiber reinforcement and polymer matrix

According to reference [29], mainly synthetic fibers, such as aramid, are subjected to photochemical degradation due to radiation above the UV B range between 280 and 315 nm. The photochemical degradation was not mentioned for glass fiber and is more critical for polymeric matrices. Thus, since this effect was small compared to polymer's degradation, no photochemical degradation of E-glass fibers was considered in current study. Glass fibers are incombustible, temperature-resistant up to a temperature of approximately 400 °C and resistant to weathering [29]. For the standard operating temperatures up to 70 °C, E-glass fibers show a slightly increase of the elastic properties [30–32]. In the current study, the elastic properties of E-glass fiber are assumed to have a constant value of E/E_0 = 1 for all investigated weathering conditions.

For the polymeric matrix, the different weathering conditions has a significant effect on the elastic modulus (Figure 4). The change of the material's temperature results in the highest change (Figure 4a). Comparing three different epoxy resins according to references [33–35], similar curve can be observed (Figure 4a). The presented data was obtained from DMA of different epoxy resins at different temperature ranges.

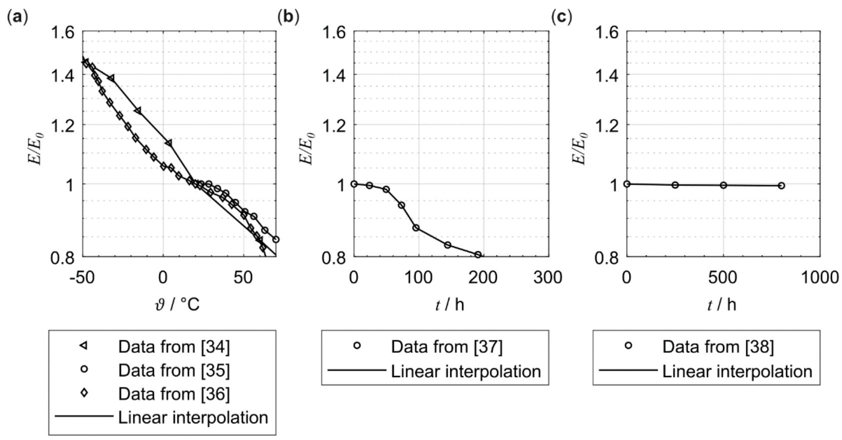

Figure 4: Elastic modulus of epoxy resin: (a) at temperatures between 20 °C and 100 °C [33–35], (b) for a certain time in a admophere with relative humidity of 60 % [36], (c) exposed to UV radiation in UV range between 200 and 400 nm and in the visible ranges between 400 and 700 nm [37].

For the numerical modeling, the measurements of Arena et al. [36] were used who analyzed the whole investigated temperature range. The absorption of moisture also influences the elastic properties of epoxy resin (Figure 4b). Comparing the individual weathering phenomena of epoxy resin, it can be seen that the influence of photochemical degradation is small compared to the other phenomena. Furthermore, it should be noted that the composite is protected against the exposure of UV radiation in the case of an unbroken coating (see Figure 2b). Only in the case of damages, small areas are exposed to UV radiation which have a considerable small influence of the structural behavior (compare Section 2.2). Due to before mentioned reasons, the photochemical degradation of epoxy resin was not further considered in the current study.

3.1 Degradation of epoxy resin

Using the changes of the resin's elastic modulus due to temperature changes (Figure 4a) and the increasing time for the absorption of moisture (Figure 4b), the resulting degradation of the polymer matrix according to Eq. (2) was determined (Figure 5). The resulting degradation at a temperature of $\vartheta = 20$ °C and at time $t = 0$ of the moisture absorptions reaches by definition a value of $(E_\mathrm{m} - E_{0,\mathrm{m}})/E_{0,\mathrm{m}} = 0$. With increasing time, the modulus decreases $(E_\mathrm{m} - E_{0,\mathrm{m}})/E_{0,\mathrm{m}} < 0$. At the upper limit of the considered temperature range of $\vartheta = -50$ °C, the elastic modulus of epoxy resin is higher than the reference value $(E_\mathrm{m} - E_{0,\mathrm{m}})/E_{0,\mathrm{m}} > 0$ (compare Figure 5). This effect is known as low temperature embrittlement in the epoxy matrix [33, 35]. It should be noted that the used damage parameter D_m is not identical to the damage parameter for the fatigue damage modelling of composite materials [28] or for biaxial load application of textile reinforced composites [38]. In the current study, only the degradation due to weathering and not to fiber or matrix damage was considered.

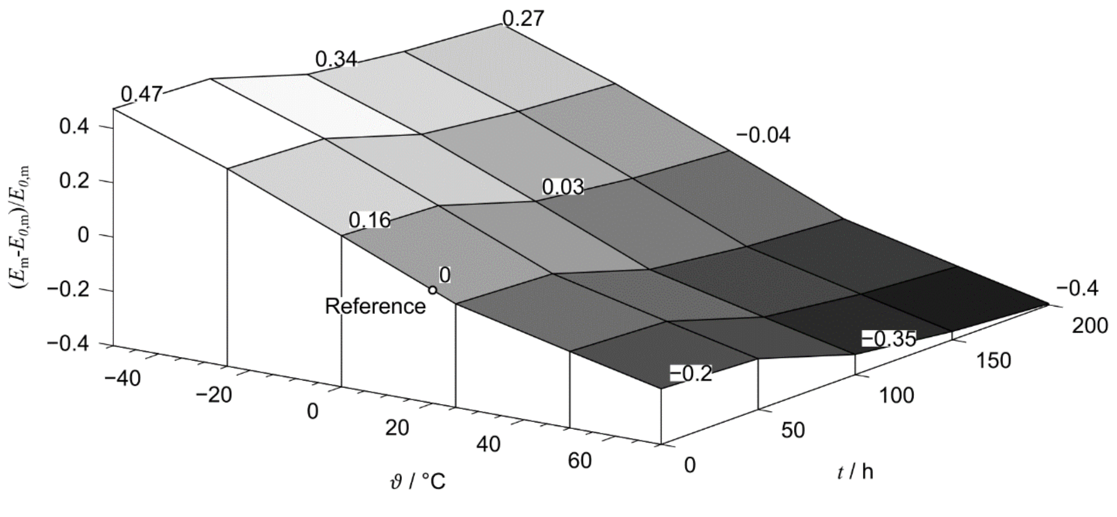

Figure 5: Resulting degradation of epoxy resin $(E_\mathrm{m} - E_{0,\mathrm{m}})/E_{0,\mathrm{m}}$ for temperatures ϑ between −50 °C and 70 °C and for a certain time t in a atmosphere with relative humidity of 60 %.

3.2 Stiffness degradation of composite

Especially the exposure to high temperatures results in a significant reduction of the tensile strength of GFRP (see e.g. [39]). This effect can be seen as result of the high temperature dependency of the polymer matrix (compare Figure 4). Additional it can be seen that due to low temperature embrittlement of epoxy resin, the elastic moduli increase as the temperature decreases (Figure 6b).

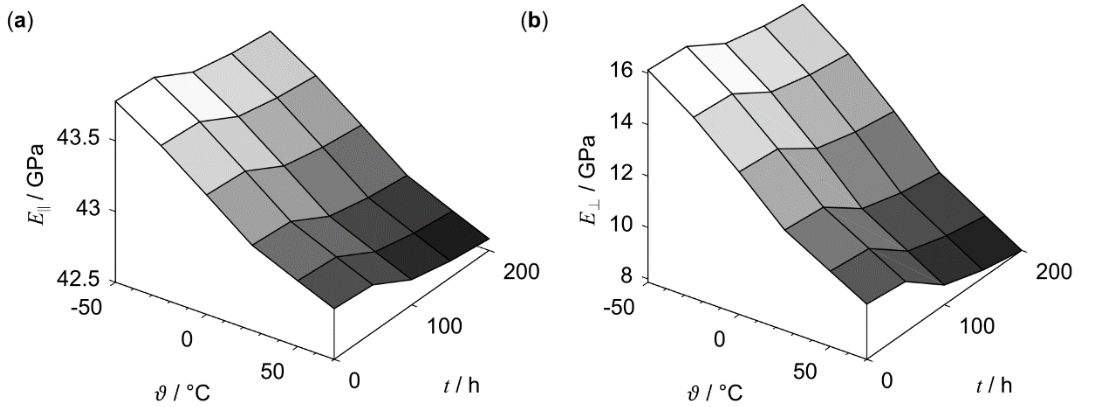

Figure 6: (**a**) Elastic modulus in fiber direction $E_{||}$ and (**b**) in transversal direction of glass fiber reinforced epoxy resin obtained from micro-scale modeling for temperatures ϑ between -50 °C and 70 °C and for a certain time t in a atmosphere with relative humidity of 60 %.

Considering all elastic constants of the investigated UD GFRP, it can be seen that especially the matrix-dominated constants, such as the transversal elastic modulus $E_{\perp}$ strongly depend on the material's temperature. The fiber-dominated elastic modulus $E_{||}$ change only slightly due to varying temperatures and the moisture absorption (Figure 7a) since the fiber properties show only very small variations for the investigated weathering phenomena (compare Section 3.1).

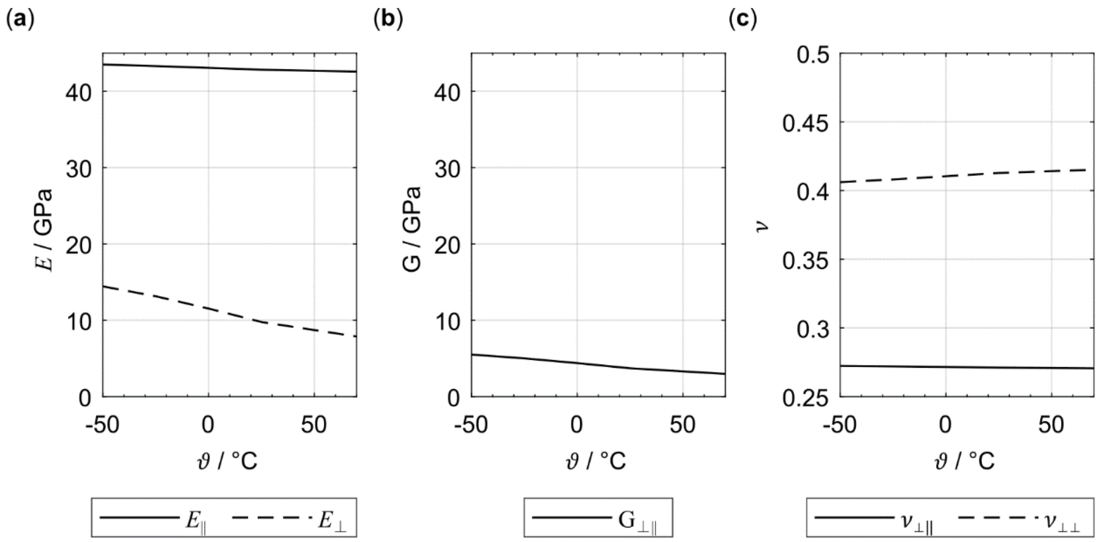

Figure 7: Degradation of the uniderectional composite's elastic moduli for temperatures ϑ between -50 °C and 70 °C after a time of t = 200 h in a atmosphere with relative humidity of 60 %: (**a**) elasticity moduli E, (**b**) shear modulus $G_{\perp||}$, (**c**) Poisson's ration ν.

3.4 Limitations and future work

The used micro-scale modeling approach enables the estimation of the composite's elastic properties according to the environmental-based degradation phenomena. In particular, the outer layers of a WTB with damaged coating are most exposed to all weathering phenomena. Currently, there are no studies that simultaneously analyze the full range of the individual dependencies of changing temperatures in the relevant range, moisture absorption and UV radiation of the elastic properties of GFRP for applications in WTBs. Investigations of the resulting effects for all combinations of weathering conditions, including also intermediate states, require a high experimental effort [10–16]. To overcome this high experimental effort, accelerated exposure tests were carried out to simulate natural weathering conditions [13, 16]. An alternative approach is the use of numerical modeling methods including RVEs to determine the individual dependencies (compare e.g. [17]). However, for this numerical approach, the complex interactions between the individual weathering phenomena and the influence on the fiber-matrix interface have to be characterized experimentally and suitable modeled. However, for the determination of the elastic properties, the component's elastic properties and a perfect bonding between the fibers and matrix material result in a good approximation of these dependencies. Nevertheless, experimental measurements are indispensable for a reliable quantification of the individual weathering effects and a micro-scale modeling. Nevertheless, the set-theoretical accumulation of the individual phenomena and the numerical micro-scale modeling approach used here provides valuable insights into the design of these experiments and can enable quantification of the maximum weathering-induced degradation of the elastic properties of GFRP as part of preliminary estimations.

4 CONCLUSIONS

The introduced micro-scale modeling approach enables a better understanding of the environmental-based natural degradation phenomena of glass fiber reinforced epoxy resin. The obtained results could be used as basis for the planning of experimental investigations. As a result of the current study, the composite elastic properties are strongly dependent on the material's temperature and the current moisture absorption. The effects of photochemical degradation are minor compared to other weathering phenomena. Overall, the finding of the current study will help to accelerate and improve the preliminary design processes of wind turbine blades by providing a first estimation of the composite's elastic properties and its degradation which will enable a preliminary quantification of new composite materials.

ACKNOWLEDGEMENTS

Funded by the European Union, within the HORIZON-CL4-2021-RESILIENCE-01 project "European recycling and circularity in large composite components (EuReComp)", call "A Digitized, Resource-Efficient and Resilient Industry 2021", HORIZON Research and Innovation Actions, Contract Number 101058089. Views and opinions expressed are however those of the author(s) only and do not necessarily reflect those of the European Union or HADEA. Neither the European Union nor HADEA can be held responsible for them.

REFERENCES

[1] L. Ziegler, E. Gonzalez, T. Rubert, U. Smolka, and J.J. Melero, Lifetime extension of onshore wind turbines: A review covering Germany, Spain, Denmark, and the UK, *Renewable and Sustainable Energy Reviews*, **82**, 2018, pp. 1261–1271 (doi: 10.1016/j.rser.2017.09.100).

[2] B. Kjærside Storm, Surface protection and coatings for wind turbine rotor blades, in *Advances in wind turbine blade design and materials* (Woodhead Publishing series in energy 47), P. Brøndsted, Ed., Oxford: Woodhead Publishing, 2013, pp. 387–412.

[3] E. Yousif and R. Haddad, Photodegradation and photostabilization of polymers, especially polystyrene: review, *SpringerPlus* (doi: 10.1186/2193-1801-2-398).

[4] A. Blaga, Weatheirng study of glass-fiber reinforced polyester sheets by scanning electron microscopy, *Polym. Eng. Sci.*, **12**, 1972, pp. 53–58 (doi: 10.1002/pen.760120109).

[5] B.F. Sørensen, J.W. Holmes, P. Brøndsted, and K. Branner, Blade materials, testing methods and structural design, in *Wind power generation and wind turbine design*, **1**, W. Tong, Ed., 2010, pp. 417–465.

[6] J. Joustra, B. Flipsen, and R. Balkenende, Structural reuse of wind turbine blades through segmentation, *Composites Part C: Open Access*, **5**, 2021, p. 100137 (doi: 10.1016/j.jcomc.2021.100137).
[7] Y. Kepir, A. Gunoz, and M. Kara, Effects of environmental conditions on the mechanical properties of composite materials, *Adv. Eng. J*, **1**, 2021, pp. 21–25.
[8] I. Rocha, S. Raijmaekers, R. Nijssen, F.P. van der Meer, and L.J. Sluys, Hygrothermal ageing behaviour of a glass/epoxy composite used in wind turbine blades, *Composite Structures*, **174**, 2017, pp. 110–122 (doi: 10.1016/j.compstruct.2017.04.028).
[9] I. Rocha *et al.*, A combined experimental/numerical investigation on hygrothermal aging of fiber-reinforced composites, *European Journal of Mechanics - A/Solids*, **73**, 2019, pp. 407–419 (doi: 10.1016/j.euromechsol.2018.10.003).
[10] A. Dogan, Y. Arman, and O. Ozdemir, Experimental investigation of transverse loading on composite panels coated with different gelcoat colors subjected to UV radiation and hygrothermal aging, *Mater. Res. Express*, **6**, 2019, p. 25301 (doi: 10.1088/2053-1591/aaeb67).
[11] M. Bazli, A. Jafari, H. Ashrafi, X.-L. Zhao, Y. Bai, and R.K. Singh Raman, Effects of UV radiation, moisture and elevated temperature on mechanical properties of GFRP pultruded profiles, *Construction and Building Materials*, **231**, 2020, p. 117137 (doi: 10.1016/j.conbuildmat.2019.117137).
[12] M. Bazli, H. Ashrafi, A. Jafari, X.-L. Zhao, R.K.S. Raman, and Y. Bai, Effect of Fibers Configuration and Thickness on Tensile Behavior of GFRP Laminates Exposed to Harsh Environment, *Polymers* (doi: 10.3390/polym11091401).
[13] K.-B. Shin, C.-G. Kim, and C.-S. Hong, Correlation of Accelerated Aging Test to Natural Aging Test on Graphite-Epoxy Composite Materials, *Journal of Reinforced Plastics and Composites*, **22**, 2003, pp. 849–861 (doi: 10.1177/0731684403022009005).
[14] S. Martins, L. Borges, and J.R. D'Almeida, Effects of Accelerated Ageing in a PTFE Matrix Polymer Composite, *Macromol. Symp.*, **299-300**, 2011, pp. 92–98 (doi: 10.1002/masy.200900163).
[15] D.E. Mouzakis, H. Zoga, and C. Galiotis, Accelerated environmental ageing study of polyester/glass fiber reinforced composites (GFRPCs), *Composites Part B: Engineering*, **39**, 2008, pp. 467–475 (doi: 10.1016/j.compositesb.2006.10.004).
[16] J.M. Sousa, J.R. Correia, and S. Cabral-Fonseca, Durability of Glass Fibre Reinforced Polymer Pultruded Profiles: Comparison Between QUV Accelerated Exposure and Natural Weathering in a Mediterranean Climate, *Exp Tech*, **40**, 2016, pp. 207–219 (doi: 10.1007/s40799-016-0024-x).
[17] L. Mishnaevsky, Micromechanical modelling of wind turbine blade materials, in *Advances in wind turbine blade design and materials* (Woodhead Publishing series in energy 47), P. Brøndsted, Ed., Oxford: Woodhead Publishing, 2013, pp. 298–324.
[18] European Wind Energy Association. “Wind in power - 2015 European statistics.” https://www.ewea.org/fileadmin/files/library/publications/statistics/EWEA-Annual-Statistics-2015.pdf (accessed Oct. 12, 2022).
[19] P. Johst, M. Kucher, P. Schulz, A. Knorr, R. Kupfer, and R. Böhm, Identification of circular eco-subsystems for end-of-life aviation composite components based on a systematized R6-strategy, *12th EASN International Conference on Innovation in Aviation and Space for opening New Horizons*, Barcelona, Spain, J. Pons i Prats, A. Strohmayer, and S. Pantelakis, Eds., 2022.
[20] K.B. Katnam, A.J. Comer, D. Roy, L.F.M. Da Silva, and T.M. Young, Composite Repair in Wind Turbine Blades: An Overview, *The Journal of Adhesion*, **91**, 2015, pp. 113–139 (doi: 10.1080/00218464.2014.900449).
[21] D.A. Katsaprakakis, N. Papadakis, and I. Ntintakis, A Comprehensive Analysis of Wind Turbine Blade Damage, *Energies*, **14**, 2021, p. 5974 (doi: 10.3390/en14185974).
[22] A. Reddy, V. Indragandhi, L. Ravi, and V. Subramaniyaswamy, Detection of Cracks and damage in wind turbine blades using artificial intelligence-based image analytics, *Measurement*, **147**, 2019, p. 106823 (doi: 10.1016/j.measurement.2019.07.051).
[23] A.S. Shihavuddin *et al.*, Wind Turbine Surface Damage Detection by Deep Learning Aided Drone Inspection Analysis, *Energies*, **12**, 2019, p. 676 (doi: 10.3390/en12040676).

[24] H. Altenbach, J. Altenbach, and R. B. Rikards, *Einführung in die Mechanik der Laminat- und Sandwichtragwerke: Modellierung und Berechnung von Balken und Platten aus Verbundwerkstoffen; 47 Tabellen*, Dt. Verl. für Grundstoffindustrie; Wiley-VCH, Stuttgart, Weinheim, 2001.
[25] H. Schürmann, *Konstruieren mit Faser-Kunststoff-Verbunden: Mit 39 Tabellen, Vol.* 2, Springer, Berlin, Heidelberg, 2007.
[26] N. N. "Ansys Material Designer User's Guide." https://ansyshelp.ansys.com/ (accessed Apr. 4, 2023).
[27] M. Schneider, The sequential addition and migration method to generate representative volume elements for the homogenization of short fiber reinforced plastics, *Comput Mech*, **59**, 2017, pp. 247–263 (doi: 10.1007/s00466-016-1350-7).
[28] H. Mao and S. Mahadevan, Fatigue damage modelling of composite materials, *Composite Structures*, **58**, 2002, pp. 405–410 (doi: 10.1016/S0263-8223(02)00126-5).
[29] G. Niederstadt, *Ökonomischer und ökologischer Leichtbau mit faserverstärkten Polymeren: Gestaltung, Berechnung und Qualifizierung, Vol.* 2, expert-Verl., Renningen-Malmsheim, 1997.
[30] E. Kessler, R. Gadow, and J. Straub, Basalt, glass and carbon fibers and their fiber reinforced polymer composites under thermal and mechanical load, *AIMS Materials Science*, **3**, 2016, pp. 1561–1576 (doi: 10.3934/matersci.2016.4.1561).
[31] W.H. Otto, Compaction Effects in Glass Fibers, *J American Ceramic Society*, **44**, 1961, pp. 68–72 (doi: 10.1111/j.1151-2916.1961.tb15352.x).
[32] J.L. Thomason, L. Yang, and R. Meier, The properties of glass fibres after conditioning at composite recycling temperatures, *Composites Part A: Applied Science and Manufacturing*, **61**, 2014, pp. 201–208 (doi: 10.1016/j.compositesa.2014.03.001).
[33] M. Arena, M. Viscardi, G. Barra, L. Vertuccio, and L. Guadagno, Multifunctional Performance of a Nano-Modified Fiber Reinforced Composite Aeronautical Panel, *Materials* (doi: 10.3390/ma12060869).
[34] D. Gibhardt, C. Buggisch, D. Meyer, and B. Fiedler, Hygrothermal Aging History of Amine-Epoxy Resins: Effects on Thermo-Mechanical Properties, *Front. Mater.*, **9**, 2022, Art. no. 826076 (doi: 10.3389/fmats.2022.826076).
[35] F. Hübner, A. Brückner, T. Dickhut, V. Altstädt, A. Rios de Anda, and H. Ruckdäschel, Low temperature fatigue crack propagation in toughened epoxy resins aimed for filament winding of type V composite pressure vessels, *Polymer Testing*, **102**, 2021, p. 107323 (doi: 10.1016/j.polymertesting.2021.107323).
[36] C. Ji, H. He, and Y. Yang, Moisture absorption process of epoxy resin and mechanical properties of its fiber composites, *Materials Testing*, **61**, 2019, pp. 23–26 (doi: 10.3139/120.111276).
[37] Saeid Nikafshar, Omid Zabihi, Mojtaba Ahmadi, Abdolreza Mirmohseni, and Mojtaba Taseidifar and Minoo Naebe, The Effects of UV Light on the Chemical and Mechanical Properties of a Transparent Epoxy-Diamine System in the Presence of an Organic UV Absorber,
[38] C. Düreth *et al.*, Determining the Damage and Failure Behaviour of Textile Reinforced Composites under Combined In-Plane and Out-of-Plane Loading, *Materials (Basel, Switzerland)* (doi: 10.3390/ma13214772).
[39] F. Yang and P. Yao, Effect of temperature on tensile mechanical properties of GFRP bars with different diameters, *IOP Conf. Ser.: Earth Environ. Sci.*, **189**, 2018, p. 32068 (doi: 10.1088/1755-1315/189/3/032068).